

# PERIPHERAL PLASMA CHARACTERISTICS IN THE URAGAN-3M TORSATRON

*A.A. Kasilov, L.I. Grigor'eva, V.V. Chechkin, A.A. Beletskii, R.O. Pavlichenko, A.V. Lozin,  
M.M. Kozulya, A.Ye. Kulaga, N.V. Zamanov, Yu.K. Mironov, V.S. Romanov, V.S. Voitsenya*

*Institute of Plasma Physics of the NSC "Kharkov Institute of Physics and Technology",  
Kharkov, Ukraine*

In the  $l=3/m=9$  Uragan-3M (U-3M) torsatron a hydrogen plasma is produced and heated by RF fields in the Alfvén range of frequencies ( $\omega \leq \omega_{ci}$ ). Peripheral plasma is investigated using two moveable Langmuir probes. Spatial distributions of plasma parameters,  $V_f$ ,  $T_e$  and  $n_e$  in two operating regimes and in three cross-sections are measured. Link between confinement volume and transition layer is shown. RF electric antenna field influence on the probes is discussed.

PACS: 52.70.Ds

## INTRODUCTION

In the  $l=3/m=9$  Uragan-3M (U-3M) torsatron a hydrogen plasma is produced and heated by RF fields in the Alfvén range of frequencies ( $\omega \leq \omega_{ci}$ ). To introduce RF power into the plasma, an unshielded frame-like antenna is used with a broad spectrum of generated parallel wavelengths [1, 2]. In the present paper, characteristics of the plasma between the last closed flux surface (LCFS) and the helical winding casings (peripheral plasma) are studied. Parameters of the peripheral plasma and running processes are closely connected with parameters and processes in the confinement volume. So, in many cases, studying characteristics and behavior of the peripheral plasma it is possible to get information about processes in the confinement volume.

Due to characteristic properties of the U-3M device, such as enclosing the whole magnetic system into a large vacuum chamber, a specific structure of the edge field lines ensuring the helical divertor magnetic configuration, and the RF method of plasma production and heating with the antenna disposed in a short section of the torus, strong toroidal and radial inhomogeneities are inherent to the peripheral plasma.

Spatial distributions of the peripheral plasma parameters (electron temperature  $T_e$  and density  $n_e$ , floating potential  $V_f$ ) in different regimes are studied with the help of Langmuir probes in the peripheral plasma in a poloidal torus cross-section far from the antenna and in two cross-sections in the region of antenna disposition, one of them crossing the area bounded by the antenna frame. The measurements are carried out in two discharge regimes [3] differing in the average density,  $\overline{n_e}$ , electron temperature, and plasma loss. As opposed to distributions of  $T_e$ ,  $n_e$  and  $V_f$  far from the antenna, absolute values of this quantities and their spatial distributions close to the antenna are subjected to strong perturbations by the near antenna field.

## 1. DEVICE DESCRIPTION AND GENERAL DISCHARGE PARAMETERS

Toroidal magnetic field  $B_\phi = 0.72$  T is generated by the helical coils only (Fig. 1). The whole magnetic system is enclosed into a  $\sim 70$  m<sup>3</sup> vacuum chamber, so an open helical divertor is realized. The frame-like

antenna (FA; 66 cm length along the torus (Fig. 2)) and a so-called three-half-turn antenna (THTA; 30 cm) are the only material objects placed between the LCFS and the helical coils. THTA is used here only for preliminary ionization before RF voltage applied to the FA. FA is symmetrically connected to the Kaskad-1 (K1) one-stage push-pull RF oscillator and d. c. isolated from the ground (vacuum chamber, helical coils).

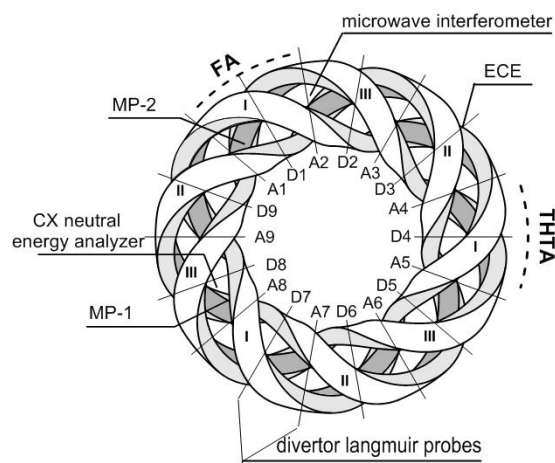


*Fig. 1. U-3M helical coils I, II, III and symmetrical poloidal cross-sections A1, D1, A2, D2, ..., A9, D9 in the helical periods 1, 2, ..., 9. Dispositions of main diagnostics, FA and THTA are indicated*

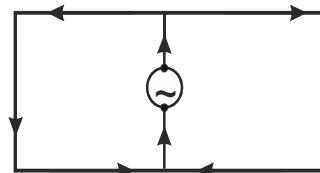


*Fig. 2. Schematic representation of the frame antenna*

RF power was changed within 45...130 kW with the K1 anode voltage changing from 5 to 9 kV. A part of this power is spent for plasma maintenance and heating in the confinement volume. Generally, plasma heating is connected with slow wave absorption by electrons [4, 5].

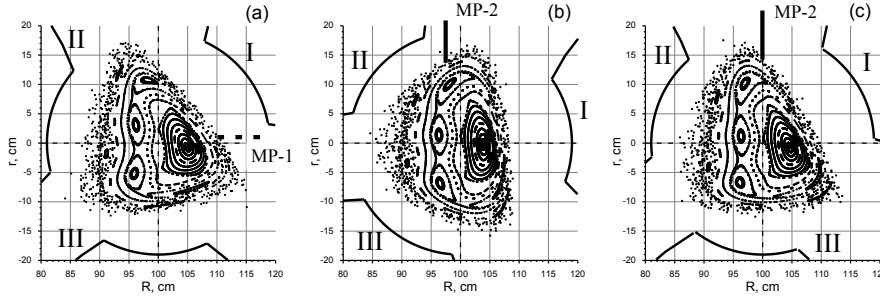


Fig. 3. Disposition of the movable probes in the poloidal cross-sections and lines of their movement (solid lines) relative to the helical coils I, II, III: (a) probe MP-1 (far from the antenna, period 8); (b) probe MP-2 (position 1 – close to the antenna, period 9); (c) probe MP-2 (period 1; position 2 – the probe crosses the area bounded by the antenna frame)

## 2. RF DISCHARGE REGIMES

In the active stage of the RF discharge two operating regimes differing by the density,  $\bar{n}_e$ , electron temperature,  $T_e^{rad}$ , and plasma loss can exist depending on the power  $P$  (voltage  $U_K$ , current  $I_{RF}$ ) and pressure  $p$ . Regime 1 is characterized by a low density  $\bar{n}_e \sim (1...3) \cdot 10^{12} \text{ cm}^{-3}$ , high electron temperature ( $T_e^{rad}$  up to 800 eV) and large plasma loss. (The latter is estimated by the value of the divertor plasma flow, DPF, which in turn is presented by the ion saturation current,  $I_s$ , to an electric probe crossed by DPF). A higher density  $\bar{n}_e \sim 7 \cdot 10^{12} \text{ cm}^{-3}$ , a lower temperature (tens eV) and low plasma loss are inherent to the regime 2. When  $U_K \sim 5...7 \text{ kV}$  regime 1 is realized in the initial stage of the discharge and then passes to the regime 2. At higher  $U_K > 7 \text{ kV}$  regime 1 persists over the entire RF pulse.

Measurements with the probe MP-2 were carried out in two poloidal cross-sections between A1 and D1 near the FA. In one experimental session the probe was moved along the vertical line at the distance 5 cm from the vertical axis of the cross-section and  $\sim 3 \text{ cm}$  from the FA edge. In this case  $V_f$ ,  $T_e$  and  $n_e$  dependencies from distance  $l$  between MP-2 and the torus midplane were measured. The probe crossed calculated LCFS at  $l \approx 16 \text{ cm}$ . During another experimental campaign the vertical line of the probe MP-2 movement was at the distance 3 cm from the vertical axis of the poloidal cross-section and crossed the area limited by the antenna frame.

$V_f$ ,  $T_e$  and  $n_e$  values were evaluated from the ion branch of the probe IV characteristic (IVC). IVCs were obtained using a 125 Hz saw-tooth generator with a  $\leq 180 \text{ V}$  negative bias voltage.

To determine the plasma parameters referred above the "ideal" dependence (see, e.g., [6])

$$I(V) = I_s \{1 - \exp[(V - V_f)/T_e]\}, \quad (1)$$

was fitted to the experimental IVC using least-squares method; where  $I(V)$  – probe current;  $V$  – bias voltage;  $I_s \approx 0,5 A n_e e (2T_e/m_i)^{1/2}$  – ion saturation current;  $A$  – probe collection area (Fig. 4).

As numerical calculations show, in all the MP-1 and MP-2 probe positions the "strong magnetic field" case,  $\rho_e < d < \rho_i$ , is realized, where  $d$  – probe diameter,  $\rho_i$  and  $\rho_e$  – ion and electron Larmor radii [6].

## 3. EVALUATION OF THE PERIPHERAL PLASMA PARAMETERS

Local peripheral plasma parameters in the region between the LCFS and helical coils were measured with movable single cylindrical langmuir probes MP-1 and MP-2 (diameter of the collection area 1 mm, length 2 mm, molybdenum) (Fig. 3). The probe MP-1 was moved horizontally from the outboard torus side between the symmetric cross-sections A8 and D8 parallel to the major radius at the distance 1 cm above the torus midplane. Dependences of  $n_e(h)$ ,  $T_e(h)$  и  $V_f(h)$  were measured, where  $h$  – the distance from the probe to the vertical axis of the poloidal cross-section where the probe is placed. The probe crossed calculated LCFS at  $h \approx 10 \text{ cm}$ .

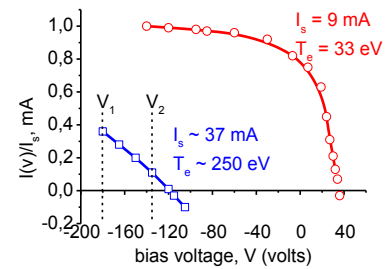


Fig. 4. Examples of experimental IVC (circles) superposed on the ideal curves calculated using Eq. (1) (lines) far (red) and close (blue) to the FA

The existence of a strong parallel RF electric field near the FA where the energy of directed motion of electrons can significantly exceed mean energy of the thermal motion leads to strong deviations from the maxwellian distribution. On the other hand, a large negative potential  $V_f$  which appears due to the rectification effect [7], complicates receiving a sufficient part of the IVC ion branch for correct estimation of  $T_e$  and  $n_e$  (see Fig. 4).

In Fig. 4 two IVCs for the regime 1 are shown as an example. One of them, typical for MP-1, allows to estimate accurately  $T_e$  and  $n_e$  using Eq. (1). Another IVC was measured with the probe MP-2 close to FA. In this case, IVC is shifted to a large negative bias  $V$ . As a result, only a small, close to straight line part of IVC is available for processing, where the fluctuation-induced scatter of the real IVC from the fitting curve could lead to strong errors in  $V_f$ ,  $T_e$  and  $n_e$  estimation. So, in assumption of the maxwellian distribution, it is possible

to talk only about some lower limit of the conventional electron temperature (mean energy)  $\sim 250$  eV.

## 4. MEASUREMENTS RESULTS

### 4.1. PERIPHERAL PLASMA FAR FROM THE ANTENNA

In Fig. 5 spatial dependencies  $V_f(h)$  (see Fig. 5,a),  $T_e(h)$  (see Fig. 5,b) and  $n_e(h)$  (see Fig. 5c,d) in the regimes I and II are shown. It is seen that at the distances from the LCFS  $12 \text{ cm} \lesssim h \leq 19 \text{ cm}$ ,  $V_f$  and  $T_e$  change slowly, within  $(-10 \dots +20 \text{ V})$  and  $(20 \dots 40 \text{ eV})$ , respectively, and  $n_e$  increases monotonically from units  $10^8 \text{ cm}^{-3}$  ( $h = 19 \text{ cm}$ ) to  $\sim 10^{10} \text{ cm}^{-3}$  ( $h = 12 \text{ cm}$ ). Closer to LCFS a sharp rise of parameters is observed in the regime I in a transition layer,  $10 \text{ cm} \lesssim h \leq 12 \text{ cm}$ , including the ergodic layer. The maximal values of  $V_f$  (up to 83 V),  $T_e$  (up to 80 eV) and  $n_e$  (up to  $6 \cdot 10^{11} \text{ cm}^{-3}$ ) are reached at  $h \approx 9.7 \text{ cm}$ . Comparing the values of plasma parameters in the transition layer in two regimes, it is seen that there is no big difference between  $V_f$  values, but maximal density in the regime II reaches  $\approx 10^{12} \text{ cm}^{-3}$  ( $h = 9.7 \text{ cm}$ ) and  $T_e$  remains on the same level as at  $h > 12 \text{ cm}$ . A further movement inside the confinement volume caused plasma perturbations (electron temperature and ECE decrease, impurity radiation increase).

During the regime I–regime II transition density increasing and temperature decreasing in the 2 cm layer boarding to LCFS represent average density and electron temperature changes in the confinement volume, thus confirming a link between plasma parameters in the confinement volume and transition layer.

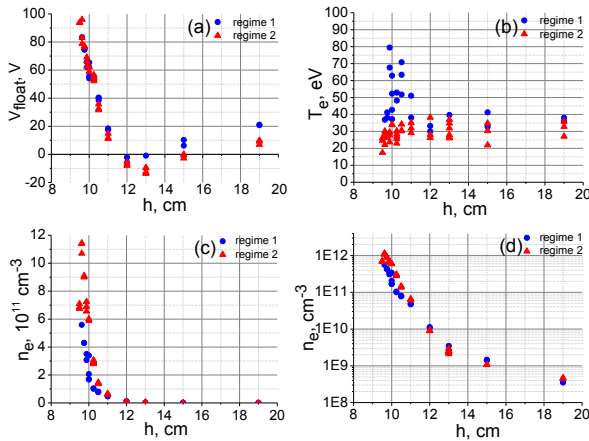


Fig. 5. Spatial distributions of plasma parameters measured using the probe MP-1 (far from the antenna). (a) – floating potential; (b) – electron temperature; (c, d) – electron density

### 4.2. PERIPHERAL PLASMA CLOSE TO THE ANTENNA

Measuring plasma parameters close to the FA, we can expect strong deviations of the values and spatial distributions of these parameters comparing with parameters far from the FA. These deviations could be caused not only because of antenna being a material object, but of stronger influence of the RF field, generated by the antenna, as well.

As it has been already mentioned above (Sec. 3), the probe MP-2 should receive a d. c. negative floating

potential due to the rectification effect in the strong electric field generated by the antenna. The value of this potential depends on the electron temperature and RF potential oscillation amplitude [7].

$V_f(h)$  dependencies, measured with the MP-2 probe in the regime I and II in the position 2, are shown in Fig. 6, a. It is seen that the values and profiles of these dependencies significantly differ from those far from FA (probe MP-1, see Fig. 5,a). At some distances the  $V_f$  values are lower than  $-100 \text{ V}$ . Particularly, the average  $V_f$  values change nonmonotonically within the range of  $(-10 \dots -140) \text{ V}$  comparing with  $(-10 \dots +80) \text{ V}$  far from FA in the regime I, and  $(0 \dots -160) \text{ V}$  comparing with  $(-10 \dots +100) \text{ V}$  far from the antenna in the regime II.

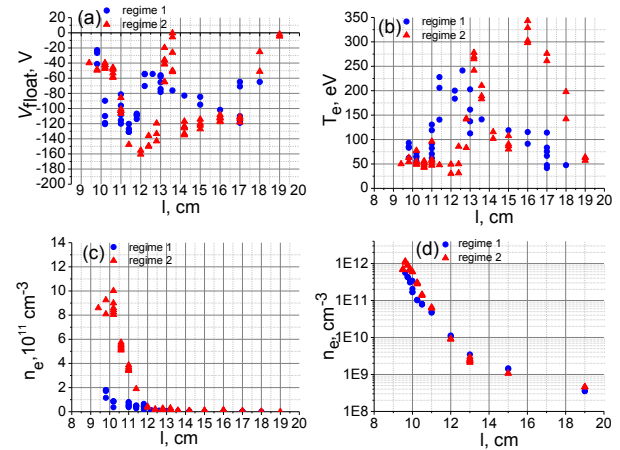


Fig. 6. Spatial distributions of plasma parameters measured using the probe MP-2 (close to the antenna, position 2). (a) – floating potential; (b) – electron temperature; (c, d) – electron density

The high negative floating potential  $V_f$  causes an IVC shift to the higher negative bias voltage  $V$ , so it is possible to get only a short, close to a straight line, part of IVC without any saturation. It is possible to evaluate  $T_e$  and  $n_e$  only at the distances  $11.5 \lesssim l \leq 13.5 \text{ cm}$ , where saturation appears. In this case we can evaluate some "efficient" electron temperature, which is noticeably higher, up to  $\sim 350 \text{ eV}$ , comparing with  $T_e \lesssim 40 \text{ eV}$  far from FA (see Fig. 5,b).

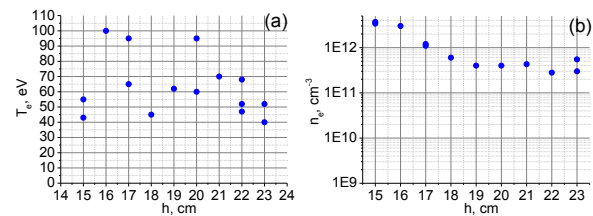


Fig. 7. Spatial distributions of plasma parameters measured using the probe MP-2 (close to the antenna, position 1) in the regime I. (a) – electron temperature; (b) – electron density

In Fig. 7  $T_e$  and  $n_e$  spatial profiles in the regime I in the position 1 are presented. In this case, higher temperature (up to  $100 \text{ eV}$ ) and density (up to  $\sim 3 \cdot 10^{12} \text{ cm}^{-3}$ ), caused by influence of the near antenna field, are also observed.

It should be noticed, that close to FA, at the distances  $10 < l < 12$  cm (transition layer), the electron temperature and density tend to return to the same values as far from FA. It means that the direct influence of the near antenna field on the plasma parameters decreases as far as  $l$  approaches  $\approx 10$  cm.

## DISCUSSION AND SUMMARY

1. A similar character of  $T_e$  and  $n_e$  variations in the transition layer and in the confinement region is observed depending on the operating regime. Such a behavior evidences interconnection between the transition layer and the confinement volume.

2. Near the antenna the values of  $V_f$  (absolute value),  $T_e$  and  $n_e$  considerably exceed those measured far from the antenna at similar distances  $h$  and  $l$ . The monotonous variations of  $n_e$  and  $T_e$  with distance observed far from the antenna are significantly broken near the antenna. Presumably, a considerable part of the RF power fed to the antenna is spent for peripheral plasma production and heating near the antenna with a further loss of this plasma.

3. Close by values plasma parameters in the transition layer far and close to the antenna allow to suppose that plasma perturbations caused by the frame antenna are damped in the transition layer and do not penetrate the confinement volume.

4. The frame antenna generates RF parallel electric field. For efficient RF power injection into the plasma and its heating the frequency and wavelength of these oscillations should be close to the frequency and

wavelength of the natural oscillations of the plasma column. Such oscillations propagate over the whole plasma torus. At the same time, in the peripheral plasma with its low density, these oscillations cannot propagate. In fact, the parallel RF electric field generated by the antenna affects the plasma similar to the near antenna field that creates strong perturbations of plasma parameters only near the antenna. In particular, a local character of these perturbations is manifested in that the density and temperature near LCFS are close to those far from the antenna. A high negative potential  $V_f$  near the antenna presumably is associated with the rectification effect in the strong RF field [7].

## REFERENCES

1. O.M. Shvets et al. // *Nucl. Fusion*. 1986, v. 26, p. 23.
2. N.T. Besedin et al. // *VIII IAEA Stellarator Workshop, Kharkov, 1991*. IAEA, Vienna, 1991, p. 53.
3. V.V. Chechkin et al. // *Plasma Physics*. 2014, v. 40, № 8, p. 697.
4. A.V. Longinov, K.N. Stepanov. *Vysokochastotnyj nagrev plazmy*. Gorkij: IPF, 1983, p. 105 (in Russian).
5. V.Ye. Golant, V.I. Fedorov. *Vysokochastotnyye metody nagreva plazmy v toroidalnykh termoyadernykh ustanovkakh*. M.: "Energoatomizdat", 1986, p. 141 (in Russian)
6. P.C. Stangeby, G.M. McCracken // *Nuclear Fusion*. 1990, v. 30, p. 1225.
7. V.A. Godyak, A.A. Kuzovnikov. О ventilnykh svojstvach VCh-razryadov // *Fizika plazmy*. 1975, v. 3 (in Russian).

Article received 10.12.2014

## ХАРАКТЕРИСТИКИ ПЕРИФЕРИЙНОЙ ПЛАЗМЫ В ТОРСАТРОНЕ УРАГАН-3М

*А.А. Касилов, Л.И. Григорьева, В.В. Чечкин, А.А. Белецкий, Р.О. Павличенко, А.В. Лозин, М.М. Козуля, А.Е. Кулага, Н.В. Заманов, Ю.К. Миронов, В.С. Романов, В.С. Войценыя*

В торсатроне Ураган-3М (У-3М) водородная плазма создается и нагревается ВЧ-полями в области альфвеновских частот ( $\omega \lesssim \omega_{ci}$ ). Периферийная плазма исследована с помощью двух подвижных ленгмюровских зондов. Пространственные распределения параметров плазмы ( $V_f$ ,  $T_e$  и  $n_e$ ) были измерены в двух режимах работы установки в трех полоидальных сечениях. Показано существование связи между областью удержания и переходным слоем. Обсуждается влияние ВЧ-электрического поля антенны на зонд.

## ХАРАКТЕРИСТИКИ ПЕРИФЕРИЙНОЇ ПЛАЗМИ В ТОРСАТРОНІ УРАГАН-3М

*А.А. Касілов, Л.І. Григор'єва, В.В. Чечкін, О.О. Білецький, Р.О. Павличенко, О.В. Лозін, М.М. Козуля, А.Є. Кулага, М.В. Заманов, Ю.К. Миронов, В.С. Романов, В.С. Войценыя*

У торсатроні Ураган-3М (У-3М) воднева плазма створюється та нагрівається ВЧ-полями в області альфвенівських частот ( $\omega \lesssim \omega_{ci}$ ). Периферійна плазма досліджена за допомогою двох рухомих ленгмюровських зондів. Просторові розподіли параметрів плазми ( $V_f$ ,  $T_e$  та  $n_e$ ) були виміряні в двох режимах роботи установки в трьох полоїдальних перерізах. Показано існування зв'язку між областю утримання та перехідним шаром. Обговорюється вплив ВЧ-електричного поля антени на зонд.